A global/local approach based on CUF for the accurate and efficient analysis of metallic and composite structures

E. Carrera[a]*, G.A. Fiordilino[a,b]†, M. Nagaraj[a]‡, A. Pagani[a]§, M. Montemurro[b]¶

[a]MUL^2, Department of Mechanical and Aerospace Engineering, Politecnico di Torino
Corso Duca degli Abruzzi 24, 10129 Torino, Italy.

[b]Arts et Métiers ParisTech, I2M CNRS UMR 5295, F-33400 Talence, France.

Submitted to: **Engineering Structures**

Author for correspondence:
E. Carrera, Professor of Aerospace Structures and Aeroelasticity,
Department of Mechanical and Aerospace Engineering,
Politecnico di Torino,
Corso Duca degli Abruzzi 24,
10129 Torino, Italy,
tel: +39 011 090 6836,
fax: +39 011 090 6899,
e-mail: erasmo.carrera@polito.it

*Professor of Aerospace Structures and Aeroelasticity, e-mail: erasmo.carrera@polito.it
†Ph.D. student, e-mail: giacinto.fiordilino@polito.it
‡Ph.D. student, e-mail: manish.nagaraj@polito.it
§Assistant Professor., e-mail: alfonso.pagani@polito.it
¶Associate professor, e-mail: marco.montemurro@ensam.eu

Abstract

The design and analysis of aerospace structures requires a detailed evaluation of stresses. Nevertheless, the complexity of large structures and the use of composite materials can significantly increase the computational costs of the models. The computational burden of such analyses can be reduced by a suitable global/local approach developed in a very general Finite Element framework. Generally, a global/local modelling approach aims at using a finer mesh in the "local" zones where a detailed evaluation of stress/strain field is required, whereas a coarse mesh is used in the rest of the structure. This work proposes a global/local methodology to set up a high-order beam model in the Carrera Unified Formulation framework only for a reduced region of the global model. The methodology makes use of two steps. In the first step, a static analysis of the global structure is done by means of a commercial software in order to identify the critical regions deserving more accurate investigations. In the second step, thus, a high-order beam model is employed for the local region based on the information from the previous global analysis. Linear elastic static analysis are considered in this work, and the attention is mainly focussed on the capability of the method to provide stable solutions and accurate 3D stress fields in the local region, even in the case of laminated composite structures. Hence, the effectiveness of the proposed approach is proven through some meaningful benchmarks.

Keywords: Global/Local Analysis, Finite Element Method, Refined Beam Theories, Unified Formulation

1 Introduction

In the aeronautical field, when dealing with the design of an aircraft structure the finite element (FE) model of the system is usually built by combining 1D and 2D elements, which opportunely discretize mathematical domains of stringers, panels, ribs, and other components. Clearly, this discretization results in a simplification of the reality. In fact, it may be necessary to determine 3D stress fields in certain regions of the model. To accurately capture these localized 3D stress fields, solid models or high-order theories are often necessary. However, in order to make the model more efficient, i.e. to balance computational cost and results accuracy, a global/local approach is often employed. Three main approaches are available in the literature to deal with a global/local analysis: (1) refining the mesh or the shape functions within critical regions [1–5]; (2) formulating multi-model methods, in which different subregions of the structure are analysed with different mathematical models [6–13]; (3) using models based on the Static Condensation also known as "Super-elements Methods" [14, 15].

The first method listed above mainly faces convergence problems in those regions where singularities occur. Adaptive techniques are often used to couple coarse and refined subregions of a structure. The *h*-adaption method [1] is used when the structure subregions differ in mesh size, whereas the *p*-adaption method [2] can be applied when the subregions differ in the polynomial order of the shape functions. Moreover, the *hp*-adaption [3] can allow the implementation of subregions differing in both mesh size and shape functions. Other techniques allowing for the coupling of different meshes are, for instance, the multi-grid method [4], and the extended finite element method (XFEM) [5]. All these methods can be addressed as single-model methods. In the case of multiple-model methods, where different subregions of the structure are modelled with kinematically incompatible elements, the compatibility of displacements and equilibrium of stresses at the interface between dissimilar elements have to be achieved. In the *s*-version of the finite element method (FEM) [6, 7], the resolution in a certain subregion of the structure is increased by superimposing additional meshes of high-order hierarchical elements. Shim *et al.* [8] combined 1D and 2D elements with 3D solid elements via multipoint constraint equations evaluated by equating the work done on both sides of the dimensional interface. In [9], the coupling of structural models with different dimensionalities was achieved by exploiting conditions derived from the governing variational principle formulated at the continuum level. Ben Dhia [11] proposed the Arlequin method to couple different numerical models. This method was adopted by Hu *et al.* [12] for the linear analysis of sandwich beams modelled via 1D and 2D finite elements.

Among the multiple-model methods, there are the so-called "Multi-steps methods" in which the analysis of the critical region requires the boundary conditions (BCs) at the interface level that are extracted by the analysis on the global structure. For instance, in the global/local method proposed by Mao *et al.* [10], a coarse mesh was used to analyse the entire structure to obtain the nodal displacements which were subsequently used as boundary conditions for the refined local analysis. According to [10], the application of the boundary conditions in the local region unavoidably introduces errors. To minimize the effect of such errors, the

local analysis generally requires a region larger than the critical region where accurate stress fields are to be evaluated. Ransom and Knight [16] presented a method for performing a global/local stress analysis. The method makes use of spline interpolation functions which satisfy the linear plate bending equation to determine displacements and rotations from a global model, which are then used as BCs for the local model. The local analysis is done in a second step and it is completely independent of the global one. This method can be used to determine detailed stress states for specific structural regions using independent, refined local models which exploit information from less-refined global models, thus reducing the computational effort.

Haryadi *et al.* presented a two-step global/local methodology to compute the static response of a simply supported composite plate with cutouts [17] and small cracks [18]. In these works, the Ritz method is used for the computations of the kinematic BCs of the local region and subsequently standard finite element method for the analysis of the local model. Their method resulted in accurate prediction of stresses with considerable computational cost savings. The work of Thompson *et al.* [19] is one of the first examples of global/local analysis from a 2D global model to 3D local one. As a first step, they realised a 2D global model of the laminate composite plate using a zooming technique to refine the mesh in the proximity of the hole to avoid the displacements interpolation in the interfaces between global/local model. In recent works [13], the Arlequin method was formulated in the context of the Carrera Unified Formulation (CUF) to couple 1D finite elements differing in the approximation order of the displacement field. The global mechanical problem was solved by merging two sub-domains via the Arlequin method. An overlapping zone was thus necessary to guarantee the structural integrity via a Lagrangian multiplier field and a coupling operator that links the degrees of freedom (DOFs) of each sub-domain within the overlapping zone. Similar results were reproduced by Carrera *et al.* [20] by coupling models with different kinematics by using point-wise Lagrange multipliers. The main difference between the Arlequin-based and the Lagrange multipliers-based variable kinematic models is that the former includes an overlapping region, in which two solutions coexist. Nevertheless, both methods are suitable for building variable kinematic models. Recently, CUF has been extended in [21] to deal with the global/local analysis of laminates by employing its intrinsic variable-kinematics capability.

A different approach is used in the case of the super-elements method where a large structure is divided into many small ones (super-elements) which are then processed individually. The processing of each super-element results in a reduced set of matrices that represent the properties of the super-element as seen at its connections to adjacent structures. The reduced matrices are computed using the static condensation by the Guyan's method [14, 15] and they are assembled with the residual structure.

This work proposes a global/local methodology that consists of a two-step procedure for the evaluation of accurate stress fields in critical regions of structures. In the proposed method, the first step is devoted to the static analysis of a global model of the structure and it could be done by commercial software using 1D/2D elements. A criterion is established to identify the most critical region, which is subsequently analyzed in the second step by using high-order models, to obtain accurate stress fields. The refined theories used in

the detailed analysis are implemented in the CUF framework. Over the last few years, CUF models have been demonstrated to be very efficient and effective for evaluating complex strain/stress fields of composite structures [22, 23] and also successful in the elastoplastic and progressive failure analyses [24, 25]. The main advantage of the proposed global/local methodology is that by exploiting the information of the static analysis on a global model composed 1D/2D elements, it is possible to obtain a detailed description of the stress field using high-order beam theories in the CUF framework in critical region of the structure, at reduced computational costs. Recently, the global/local methodology has been extended to the elastoplastic analysis of compact and thin-walled structures via refined models [26] and following works may address localized buckling analysis and global/local optimization processes for aerospace structure design. Figure 1 shows some of the possible applications of the proposed global/local methodology.

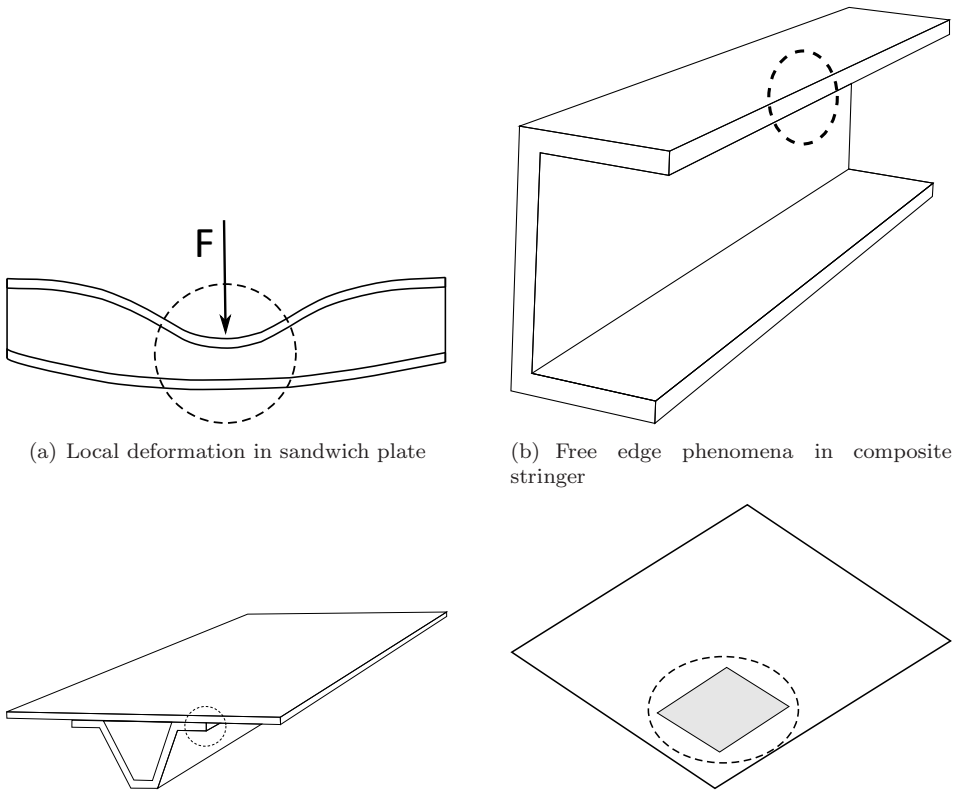

(a) Local deformation in sandwich plate

(b) Free edge phenomena in composite stringer

(c) Delamination in composite plate

(d) Local optimization

Figure 1: Examples of applications of the global/local *CUF* methodology

This paper is structured as follows: a brief introduction of 1D models based on the CUF is given in Section 2, followed by a description of the global/local methodology in Section 3, where the application of BCs and coupling effects are also discussed. In Section 4, meaningful benchmarks are presented to assess the validity of the proposed global/local methodology. Finally, the conclusions of this work are presented in Section 5.

2 1D models based on the Unified Formulation

Consider a generic beam structure whose longitudinal axis, with respect to a Cartesian coordinate system, lies on the coordinate y and its cross-section is defined on the xz-plane, as shown in Fig. 2.

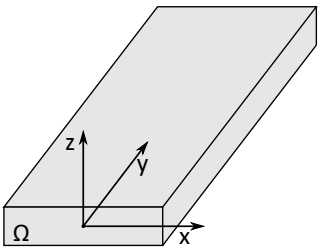

Figure 2: Coordinate frame of the beam model

Let us introduce the transposed displacement vector, $\mathbf{u}^T(x,y,z) = \{u_x(x,y,z), u_y(x,y,z), u_z(x,y,z)\}$. The cross-section of the structure is denoted by Ω, and the beam boundaries over y are $0 \leq y \leq L$. The strain $\boldsymbol{\epsilon}$ and stress $\boldsymbol{\sigma}$ components are arranged according to the Voigt's notation as:

$$\begin{aligned} \boldsymbol{\epsilon}^T &= \Big\{\epsilon_{xx} \quad \epsilon_{yy} \quad \epsilon_{zz} \quad \epsilon_{yz} \quad \epsilon_{xz} \quad \epsilon_{xy}\Big\}, \\ \boldsymbol{\sigma}^T &= \Big\{\sigma_{xx} \quad \sigma_{yy} \quad \sigma_{zz} \quad \sigma_{yz} \quad \sigma_{xz} \quad \sigma_{xy}\Big\}. \end{aligned} \tag{1}$$

In the case of small displacements with respect to a characteristic dimension the strain - displacement relations are

$$\boldsymbol{\epsilon} = \boldsymbol{D}\mathbf{u}, \tag{2}$$

where $\boldsymbol{D}$ is the linear differential operator. The stress components can be attained by means of the Hooke's law

$$\boldsymbol{\sigma} = \boldsymbol{C}\boldsymbol{\epsilon}, \tag{3}$$

where $\boldsymbol{C}$ stiffness matrix of the material. For the sake of brevity matrices $\boldsymbol{D}$ and $\boldsymbol{C}$ are not reported here but they can be easily found in [27].

According to CUF, the displacement field over the cross-section can be expressed as follow:

$$\mathbf{u}(x,y,z) = F_\tau(x,z)\mathbf{u}_\tau(y), \qquad \tau = 1,2,....,M\ , \tag{4}$$

where F_τ vary over the cross-section, $\mathbf{u}_\tau$ is the generalized displacement vector and M stands for the number of terms of the expansion where the repeated subscript, τ, indicates summation.

The choice of F_τ determines the class of the 1D CUF model that has to be adopted. In this paper, F_τ are Lagrange Expansions (LE) which are based on the use of Lagrange polynomials as generic functions above the cross-section. The cross-section is divided into a number of local expansion sub-domains, whose polynomial

Point	α_τ	β_τ
1	-1	-1
2	0	-1
3	$+1$	-1
4	$+1$	0
5	$+1$	$+1$
6	0	$+1$
7	-1	$+1$
8	-1	0
9	0	0

Table 1: L9 cross-section element point natural coordinates

degree depends on the type of Lagrange Expansion employed. Three-node linear L3, four-node bilinear L4, nine-node cubic L9, and sixteen-node quartic L16 polynomials can be used to formulate refined beam theories. LE allows for taking into account arbitrary section geometries. Fig. 3, shows the point locations of one L9 sub-domain and Tab. 1 reports the point natural coordinates. In the case of a L9 element the interpolation functions are given by:

$$
\begin{aligned}
F_\tau &= \tfrac{1}{4}(\alpha^2+\alpha\alpha_\tau)(\beta^2+\beta\beta_\tau), \qquad \tau = 1,3,5,7\ , \\
F_\tau &= \tfrac{1}{2}\beta_\tau^2(\beta^2+\beta\beta_\tau)(1-\alpha^2) + \tfrac{1}{2}\alpha_\tau^2(\alpha^2+\alpha\alpha_\tau)(1-\beta^2), \qquad \tau = 2,4,6,8\ , \\
F_\tau &= (1-\alpha^2)(1-\beta^2), \qquad \tau = 9\ ,
\end{aligned}
$$

where α and β vary between -1 and $+1$. In the case of L9 polynomials, the displacement field reads:

$$
\begin{aligned}
u_x &= F_1 u_{x1} + F_2 u_{x2} + F_3 u_{x3} + F_4 u_{x4} + F_5 u_{x5} + F_6 u_{x6} + F_7 u_{x7} + F_8 u_{x8} + F_9 u_{x9}, \\
u_y &= F_1 u_{y1} + F_2 u_{y2} + F_3 u_{y3} + F_4 u_{y4} + F_5 u_{y5} + F_6 u_{y6} + F_7 u_{y7} + F_8 u_{y8} + F_9 u_{y9}, \\
u_z &= F_1 u_{z1} + F_2 u_{z2} + F_3 u_{z3} + F_4 u_{z4} + F_5 u_{z5} + F_6 u_{z6} + F_7 u_{z7} + F_8 u_{z8} + F_9 u_{z9},
\end{aligned}
$$

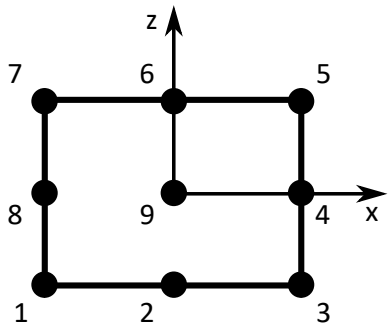

Figure 3: L9 expansion on the beam cross-section.

Refined beam models can be obtained by adopting high-order Lagrange polynomials or by using a combination of Lagrange polynomials on multi-domain cross-sections, e.g. in Fig. 4 three assembled L9 polynomial expansion sub-domains are represented. More details about Lagrange-class models can be found in [23, 27] For the sake of clarity, thanks to the multi-domain nature of the LE models, *Layer - Wise* models can be

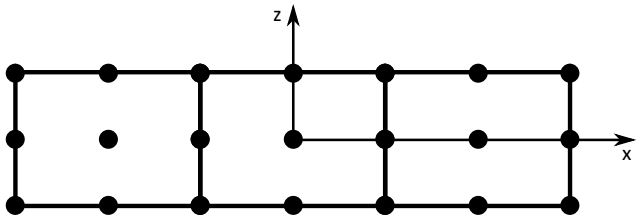

Figure 4: Three assembled L9 expansions.

implemented straightforwardly by considering one or several local expansions for each layer in the case of composite structures.

In order to discretise the structure along the y-axis, the *Finite Element Method* is adopted. This process is conducted via a classical finite element technique, where the generalized displacement vector $\mathbf{u}_\tau(y)$ can be approximated by the nodal shape functions $N_i(y)$.

$$\mathbf{u}(x,y,z) = N_i(y)F_\tau(x,z)\mathbf{u}_{i\tau}, \qquad \tau = 1,...,M, \qquad i = 1,...,n_n, \tag{5}$$

where $N_i(y)$ stands for the $i-th$ shape function, n_n is the number of nodes in one element and $\mathbf{u}_{i\tau}$ is the vector of nodal unknowns. For the sake of brevity, the shape functions are not reported here. They can be found in classical books as, [3]. Elements with four nodes (B4) are adopted in this work, in this way a cubic approximation along the y-axis is assumed. The correspondent virtual variation of the displacement can be written as:

$$\delta\mathbf{u}(x,y,z) = N_j(y)F_s(x,z)\delta\mathbf{u}_{js}, \qquad s = 1,...,M, \qquad j = 1,...,n_n. \tag{6}$$

The governing equations are derived by applying the Principle of Virtual Displacements (PVD). For a static problem:

$$\delta L_{int} = \delta L_{ext}, \tag{7}$$

where δL_{int} stands for the virtual variation internal work, δL_{ext} is the virtual variation of work done by the external loads. The virtual variation of the internal work can be expressed as:

$$\delta L_{int} = \int_V \delta\boldsymbol{\epsilon}^T\boldsymbol{\sigma}dV. \tag{8}$$

By using Eq. 2, 3 and 5 the previous expression simplifies to:

$$\delta L_{int} = \delta\mathbf{u}_{js}^T\mathbf{K}^{ij\tau s}\mathbf{u}_{i\tau}, \tag{9}$$

where $V = \Omega\cdot L$ is the volume of the beam and $\mathbf{K}^{ij\tau s}$ is the stiffness matrix in the form of a 3×3 fundamental nucleus (FN). The derivation FN is not reported here, but for the sake of completeness, it is described in [23].

However, the terms $K_{xx}^{ij\tau s}$ and $K_{xy}^{ij\tau s}$ are given for clarity purpose.

$$\begin{aligned} K_{xx}^{ij\tau s} = & \ (\lambda + 2G) \int_L N_i N_j \, dy \int_\Omega F_{\tau,x} F_{s,x} \, d\Omega + G \int_L N_i N_j \, dy \int_\Omega F_{\tau,z} F_{s,z} \, d\Omega + \\ & + G \int_L N_{i,y} N_{j,y} \, dy \int_\Omega F_\tau F_s \, d\Omega, \\ K_{xy}^{ij\tau s} = & \ \lambda \int_L N_{i,y} N_{j,y} \, dy \int_\Omega F_\tau F_{s,x} \, d\Omega + G \int_L N_i N_j \, dy \int_\Omega F_{\tau,x} F_s \, d\Omega, \end{aligned} \tag{10}$$

where G and λ are the Lamé's parameters and comma denotes partial derivatives. It can be proven that all the components of $\mathbf{K}^{ij\tau s}$ can be derived from Eq. 10 by permutations. Furthermore, it should be noted that the formal expressions of the components of the fundamental nucleus $\mathbf{K}^{ij\tau s}$ of the stiffness matrix do not depend on the choice of the cross-sectional functions F_τ, which determine the theory of structure, and shape functions N_i, which determine the numerical accuracy of the FEM approximation. This means that any classical or high-order beam element can be automatically formulated by opportunely expanding the fundamental nuclei according to the indexes τ, s, i, and j.

The formal expression of the load vector coherent to the considered model and theory can be found in [27].

3 Global/local methodology in the CUF framework

The primary objective of this study is the assessment of a global/local modelling strategy, in CUF framework. This global/local approach is useful when complex and localized stress fields have to be computed in complex structural models. Solid models are generally required to capture these localised stress fields but global/local approaches based on CUF can be used to make the analysis computationally efficient.

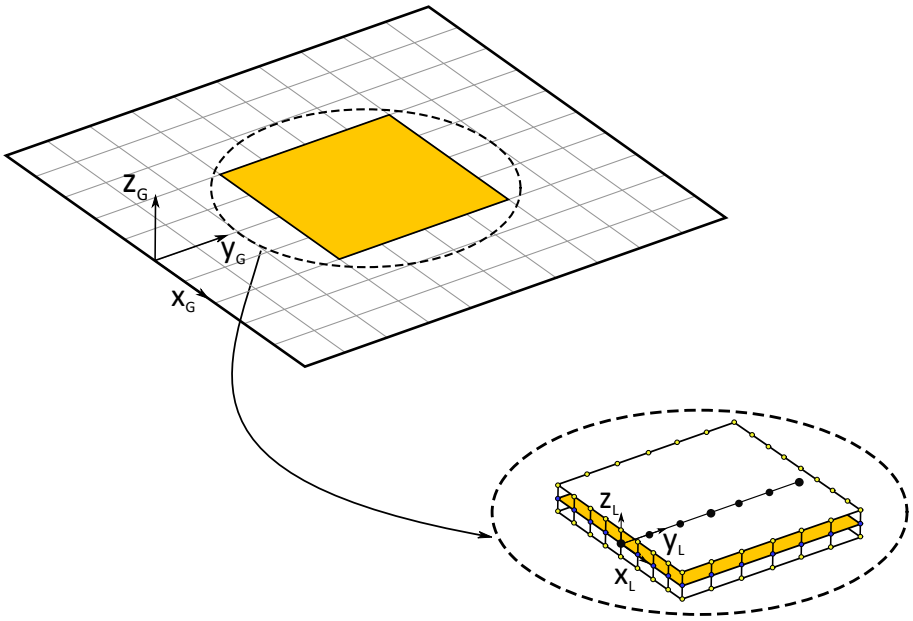

Figure 5: Global plate model and the isolated critical region

The considered global models are built by using 1D, 2D or a combination of 1D and 2D elements and they are realized by commercial software. In general, such models are low-fidelity models involving low computational costs, thus they are not suited to determine complex stress fields (e.g. out-plane stresses), due to the hypotheses at the basis of the associated kinematic model. The idea of the global/local approach developed in the CUF framework is to identify the critical regions in the global models, to isolate them and to set up CUF high-order beam models for detecting complex stress fields with very good level of accuracy and a reduced computational effort in localized and critical areas.
The proposed methodology consists of two-steps. The first step involves the analysis of the global model to identify the critical region using a criterion that is established by the analyst and to extract a proper set of BCs to be applied to the local model which is analysed with CUF. At this stage, two important questions arise:

1. What type of BCs have to be transferred from the global to the local model? Two types of BCs are discussed in the following: *Mechanical-BCs* and *Geometrical-BCs*

2. How to couple the global model realized in commercial software to the local one realized in CUF framework, which are intrinsically inconsistent? This is an interesting problem because the CUF 1D elements are kinematically different from those available in commercial software.

The above points are elaborated in the following sections. The second step of the methodology is devoted to the setting of a CUF local model and the related local static analysis. For instance, in Fig. 5, a global model of a plate is shown along with local critical region and the associated local *CUF* model.

3.1 Application of boundary conditions

The global/local coupling can be made by applying two types of BCs, i.e. *Mechanical BCs* and *Geometrical BCs*.

- *Mechanical BCs*

  The application of forces and moments at the interface makes the FE static problem indeterminate. The structure is unconstrained, and consequently, its stiffness matrix is singular. These kind of problems are frequent in the aerospace field and they are solved by making use of a procedure known in the literature as *Inertia relief*, [28–31]. This procedure, implemented by commercial software as *MSc-Nastran* and *Abaqus CAE*, allows to simulate unconstrained structures in static and dynamic analysis. In fact, taking into account the rigid body motions of the structure, it removes the singularity of the stiffness matrix so the final algebraic system could be solved. For a deeper insight in the matter the interested reader is addressed to [29, 30].

- *Geometrical BCs*

  The application of displacements and rotations at interface does not require further procedures because the system is constrained, resulting in a determinate problem that can be solved. This is the reason for the prevalence of *Geometrical BCs* in the majority of global/local approaches, see [10, 16, 19].

The *Geometrical - BCs* will be applied in the local *CUF* models for the numerical results of this work.
Figure 6 shows a plate model to be analysed with the global/local approach. The static analysis on the entire structure is done by a commercial software, and the displacements and rotations at the interface nodes are known. For the sake of simplicity, consider two structural nodes A and B, located at the interface between the global model and the critical region, as shown in Fig. 6(a). Exploiting the displacements and rotations of the nodes A and B and using linear shape functions, it is possible to determine for all the middle plane nodes of the CUF local model located nodes A and B the value of both displacements and rotations, as illustrated in Fig. 6(b). A linear interpolation function is used to maintain conformity with the kinematics of the global model. Furthermore, such interpolation procedures allow the use of the global and local meshes, which are incompatible at the interface.
Once the displacements and rotations are computed at the interface nodes located on the middle plane of the local *CUF* model, a strategy is needed to compute the BCs in all the nodes at the interface level. As known, the commercial software gives translational displacements (u_x, u_y, u_z) and rotations (θ_x, θ_y, θ_z) at the interface nodes in the case of beam and plate models. On the other hand, the use of Lagrange polynomials in CUF results solely in pure displacement degrees of freedom (DOFs) at each node. Therefore, a strategy must be provided to transform rotational DOFs of the global model in pure displacements for CUF local one. The above issue can be resolved via two approaches based on the type of elements of the global model. Reissner - Mindlin displacement field is used when the global model is a 2D model, in order to compute the translational displacements for each node at the interface of the *CUF* local model. The Reissner - Mindlin displacement field is reported in Eq. 11.

$$\begin{aligned} u(x,y,z) &= u_0(x,y) + z\theta_y(x,y), \\ v(x,y,z) &= v_0(x,y) - z\theta_x(x,y), \\ w(x,y,z) &= w_0(x,y). \end{aligned} \tag{11}$$

When the global model is a 1D model, Timoshenko displacement field Eq. 12 is used.

$$\begin{aligned} u(x,y,z) &= u_0(y), \\ v(x,y,z) &= v_0(y) + x\theta_z(y) - z\theta_x(y), \\ w(x,y,z) &= w_0(y). \end{aligned} \tag{12}$$

Where u_0, v_0, w_0 are the displacements and θ_x, θ_y, θ_z are the rotations of the nodes of the global model located

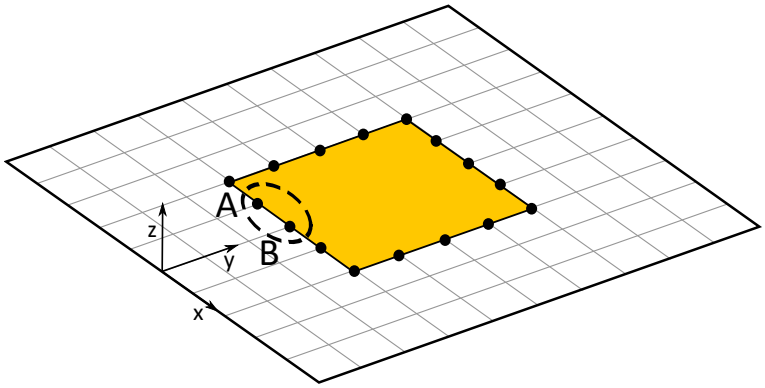

(a) Global and local regions

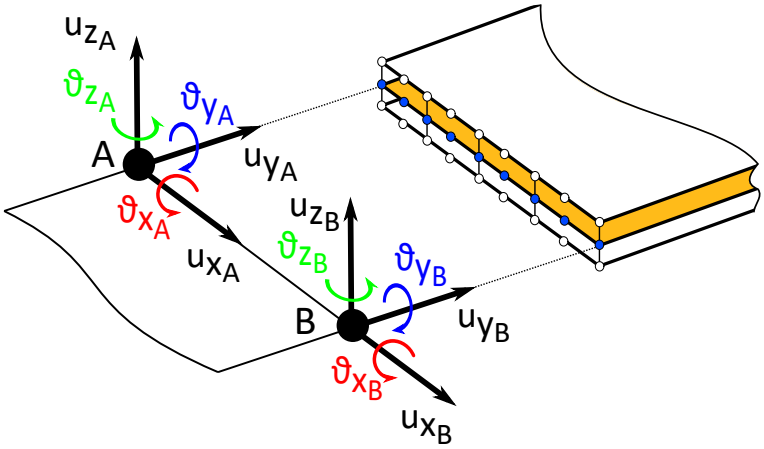

(b) Global to local

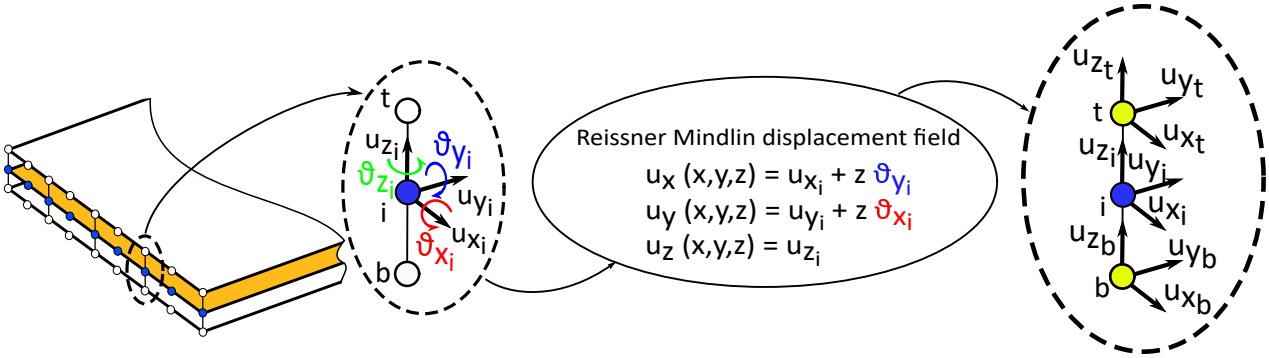

(c) Kinematics from global to local

Figure 6: Application of geometrical BCs.

at the interface. In both cases, the rotations are used to compute displacements in all the cross-section nodes at the interface level and the resulting displacements constitute the BCs for the local model.

For instance, in Fig. 6(c), the displacements and rotations computed at the node 'i' give the translational displacement at the nodes 't' and 'b' through the use of the Reissner - Midlin displacement field. In this way, it is possible to obtain from the displacements and rotations in the middle plane the translational displacements in all the nodes at the interface level.

3.2 Coupling effects

As shown in the work of Mao *et al.* [10], the application of the boundary conditions at the interface level introduces detrimental effects in the accuracy of the solution of the local static problem.
There are several strategies available to reduce these effects. In this paper the following techniques are used:

- Once the critical local region is identified, a transition zone is considered which surrounds the actual local region, as shown in Fig. 7. The displacements and rotations are applied on the nodes located at the edge of this zone following the strategy described in the previous section.

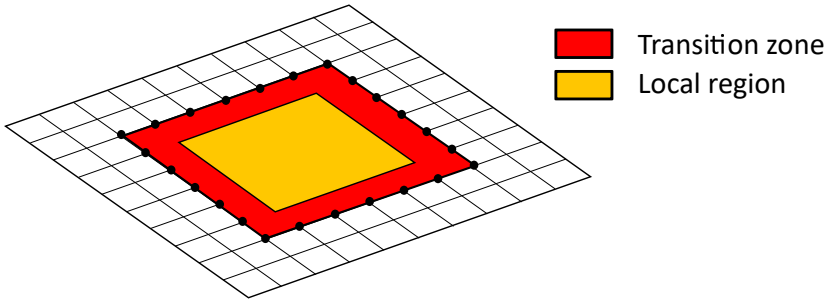

Figure 7: Global and local regions with the transition zone

- A mesh local refinement is adopted to confine the detrimental effects of the BCs application into the interface zone. This strategy consists of a non-uniform mesh in which the structural nodes and the sub-domain expansion points along x-axis are distributed with the square root of the well-know *Chebyshev* node formula. For instance, the sub-domain expansion points along x-axis are computed as:

$$x_k = \sqrt{\cos(\frac{2k-1}{2n}\pi)}, \qquad k = 1, ..., n_x. \tag{13}$$

  Where n_x is a positive integer computed from the number of sub-domains $N_{x_{exp}}$ used for the cross-section of the local *CUF* model along the x-axis, $n_x = 2 \cdot N_{x_{exp}} - (N_{x_{exp}} - 1)$. Using the previous node formula, the mesh of the local *CUF* model is refined in the proximity of the BCs. In this way, it is possible to limit the detrimental effects of the BCs only in this more refined zone. Instead, the sub-domain expansion points along z-axis are equally spaced. Figure 8(a) shows an example of the cross-section for a local model in which the point distribution follow the Eq. 13 instead in Fig. 8(b) the correspondent beam local model in the *CUF* framework is presented. In both the images, it is possible to remark the refinement in the proximity of the boundaries of the model to confine the detrimental effects of the displacements application.

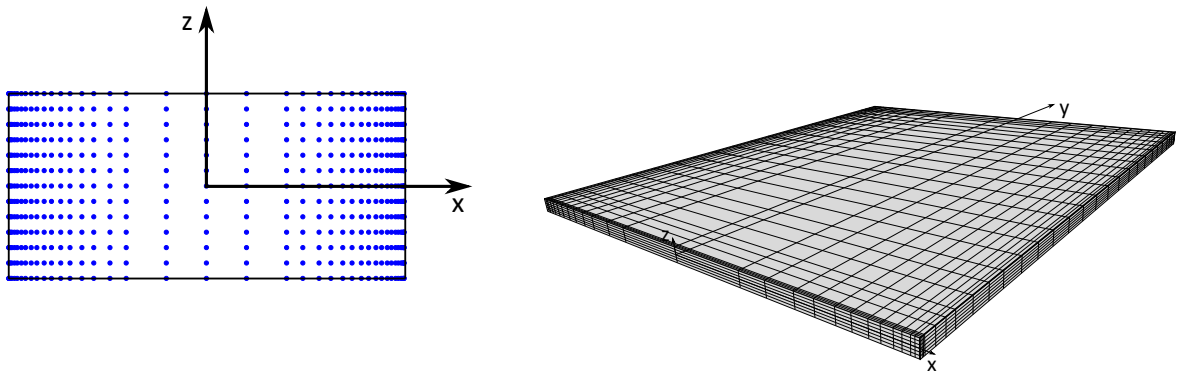

(a) Local cross-section refinement (b) Local plate region in *CUF* framework

Figure 8: Mesh refinements to decrease the detrimental effect of application of BCs

4 Numerical results

Various benchmarks related to metallic and composite structures have been solved to prove the effectiveness of the proposed method.

4.1 Cantilever beam with a point load at the free edge

This first example is done to explain and to demonstrate the ability of the proposed methodology in detecting an accurate 3D stress field, at a reduced computational cost. A cantilever beam is considered in this first case. The rectangular cross-section is characterized by $b = 1.0\ mm$, $h = 10.0\ mm$ and the beam length L is $90.0\ mm$ as illustrated in Fig. 9. An isotropic material is used for the structure with Young's modulus $E = 75$ GPa, Poisson ratio, $\nu = 0.33$ and density, $\rho = 2700\ kg/m^3$.

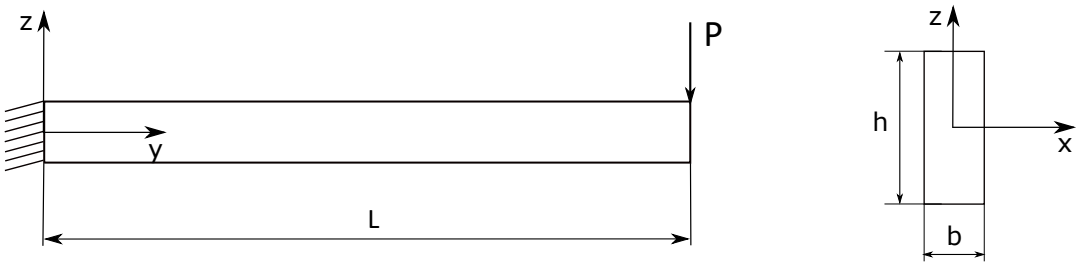

Figure 9: Geometrical features of the cantilever beam

A point load P along z-axis is applied at the free edge of the beam at [0, L, 0] and its magnitude is equal to $-1\ N$. The local region on the structure is shown in Fig. 10, whose domain extends between points A = [0, 30, 0] mm and B = [0, 60, 0] mm in the global reference system. A 'monolithic' beam model is set in the commercial software MSc Nastran using 30 1D-beam elements. A preliminary static analysis of this model gives the displacements and rotations (geometrical BCs) at the boundary nodes of the local region. In the second step, a *CUF* local beam model is set for the local region applying the geometrical BCs.

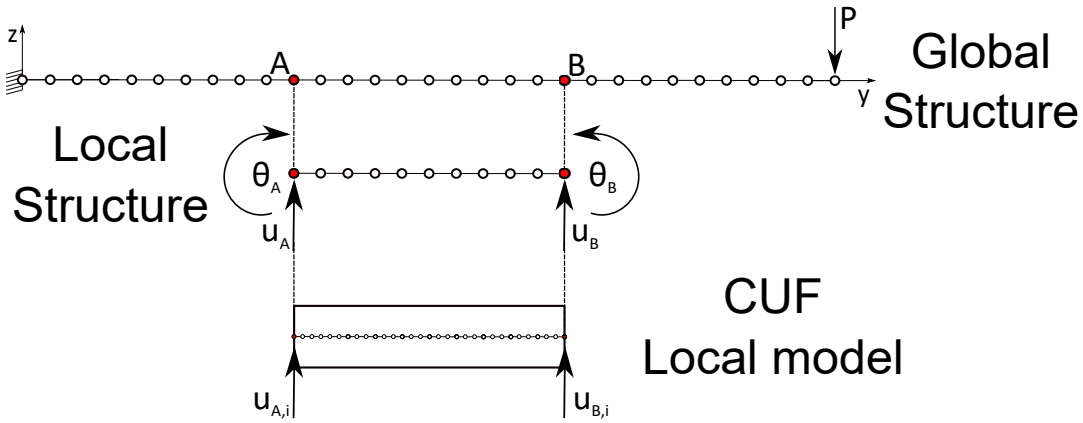

Figure 10: Global and local structure for the cantilever beam static analysis

In Fig. 10, the displacements u_{A_i} and u_{B_i} are the generic traslational displacements of the cross section 'i' point. They are computed with Timoshenko's displacement field exploiting the vertical displacements (u_A and u_B) and rotations (θ_A and θ_B) of the static analysis in the global model.

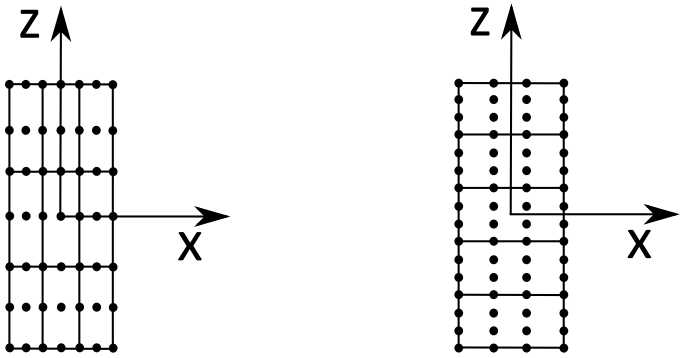

(a) 3 x 3 L9 (b) 1 x 5 L16

Figure 11: Sub-domain distributions over the cross-section of the local *CUF* beam model

Two different CUF models have been used in the global/local approach: 3x3 L9 and 1x5 L16, where 3x3 L9 means that three subdomains L9 are used along the x-axis and three along the z-axis, in the second global/local model 1 L16 subdomain along x and five subdomains L16 along z. For both the CUF models, 10 B4 elements are used for the structural mesh along y-axis. The sub-domains over the cross-section of the aforementioned CUF local models are reported in Fig. 11. Figure 12 shows the distribution of the shear σ_{yz} along the y-axis in $x = 0, z = h/2$ comparing: a Timoshenko beam model, a 3D *MSc-Nastran* model and two global (*MSc Nastran 1D*)/local (*CUF*) models with geometrical BCs.

Table 2 and Fig. 13 show the comparison between the monolithic 3D model and the global/local models in terms of axial stress σ_{yy} and shear stress σ_{yz}. The distributions of Fig. 13 are computed at $x = 0$, $y_{global} = 45.0$ $[mm]$ and the stress values, which are reported in Table 2, are at the z coordinate that gives the maximum value of these stress.

	σ_{yy} $[MPa]$	σ_{yz} $[MPa]$	DOFs
Monolithic ABAQUS 3D	2.571	-0.148	14209
NASTRAN 1D / CUF - 3x3 L9	2.721	-0.149	546 / 4557
NASTRAN 1D / CUF - 1x5 L16	2.717	-0.153	546 / 6054

Table 2: σ_{yy} and σ_{yz} for the cantilever beam with a point load

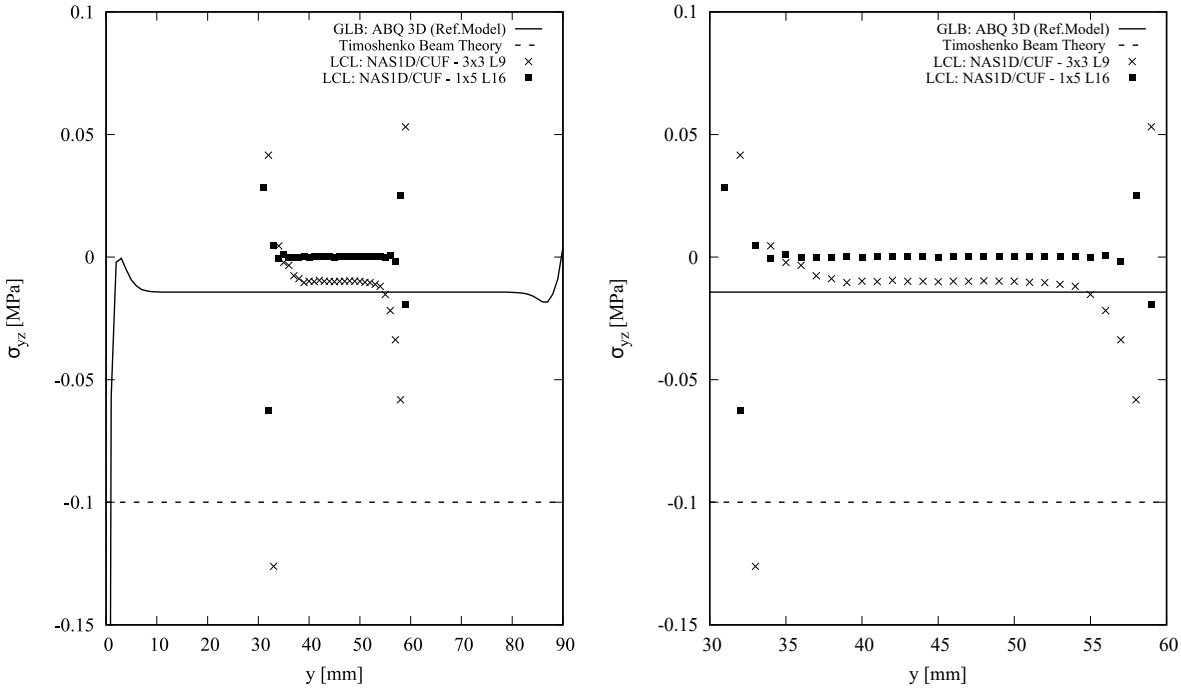

(a) σ_{yz} along the y axis in the global reference

(b) σ_{yz} along the y axis in the local reference

Figure 12: Shear σ_{yz} distribution along the y axis at the top of cross-section

The following remarks can be inferred from this preliminary analysis:

- The global/local analysis permits to detect 3D stress field reducing the computational cost of the model. In fact, it is known from theory of elasticity that the shear stress σ_{yz} has to be null at the top and the bottom of the cross-section for the equilibrium but this result can not be obtained with a 1D model and not even with a full 3D model in which the σ_{yz} is computed but it is not zero. With CUF high-order beam model, it is possible to obtain nearest null shear σ_{yz} stress at the top and the bottom of the cross-section.

- The global/local model, after an initial oscillation that is due to the BCs application, can detect a nearest null shear stress σ_{yz}. It is important to isolate a suitable region for local analysis, since the application of BCs can affect the accuracy of results. It is recommended to consider a larger area for the local analysis by including a transition zone around the critical region in order to avoid the detrimental effects of BCs application.

- Table 2 compares the axial and shear stresses obtained via monolithic and global/local analyses. All the global/local model results present good confidence with the monolithic Nastran 3D model, which

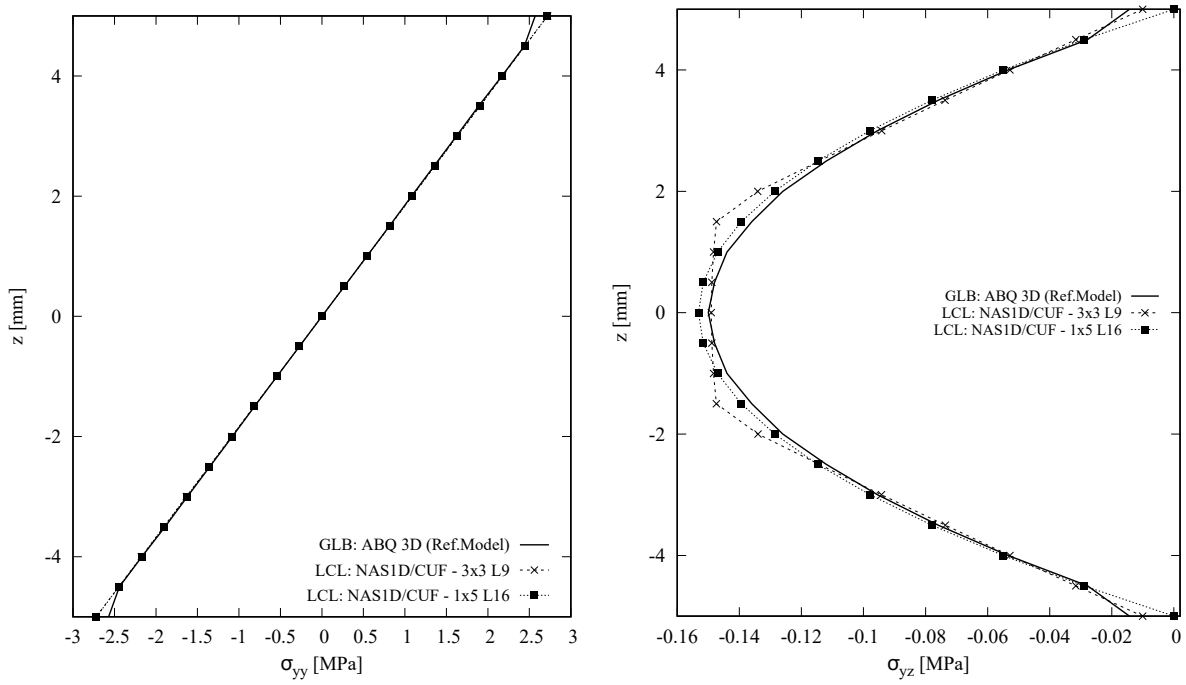

(a) Axial stress σ_{yy}

(b) Shear stress σ_{yz}

Figure 13: Axial σ_{yy} and shear σ_{yz} distribution along the z axis at $x_{global} = 0$ $[mm]$, $y_{global} = 45.0$ $[mm]$ for the cantilever beam

constitutes a numerical reference solution. The significant achievement is the reduction of the computational cost and the possibility to detect the shear stress correctly with a high-order beam model that is set with BCs that come from a lower order beam model done by commercial software.

- Figure 13 shows the stress distribution through the thickness at $y_{global} = 45.0$ mm . There are no remarkable differences for the axial stress σ_{yy}, however in the case of shear stress σ_{yz}, it can be noticed that only the global/local model with 1x5 L16 subdomains can detect a close to zero stress at the top and bottom of the cross-section, as predicted by the theory.

4.2 Isotropic plate under bending

An isotropic square plate is considered in this example. The plate is characterized by a width $b = 1.0$ $[m]$ and a thickness $t = 0.01$ $[m]$. An isotropic material is used for the structure with $E = 75$ GPa, Poisson's ratio, $\nu = 0.33$ and density, $\rho = 2700$ $\frac{kg}{m^3}$. The plate is clamped on each side and a pressure $P = 1$ Pa is applied at the top surface of the plate.

Figure 14 shows the global and the local regions of the plate and highlights points A and B in which the in-plane and out-plane stresses are evaluated, respectively. The global analysis is performed in *Msc-Nastran* and consists of 60 x 60 plate elements (DOFs = 22326). The boundaries of the local region are: $-0.167 \leq x \leq 0.167$ m and $0.300 \leq y \leq 0.700$ m; point A is located in the middle of the plate ($x_A = 0.00$ m and $y_A = 0.500$ m) and point B is located at $x_B = 0.050$ m and $y_B = 0.550$ m.

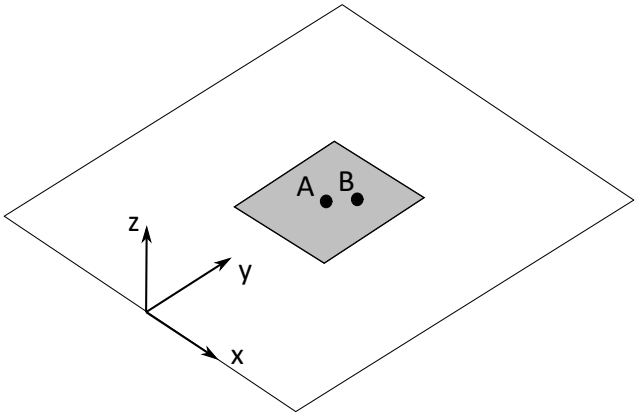

Figure 14: Global and local regions of the isotropic plate under bending

An ABAQUS solid model is build as a reference for the in-plane and out-plane stresses and it consists on 100 x 100 elements in plane and 10 through the thickness of the plate (DOFs = 855393). The local 1D model set in CUF framework consists of 20 B4 structural elements and 10 x 9 L9 sub-domains across the cross-section of the beam model (DOFs = 107787). In Fig. 15 the structural mesh of the beam axis and the distribution of the L9 over the cross-section are presented. It is noteworthy that the distributions of the structural nodes of the beam axis and the points of the L9 sub-domains of the cross-section follow the square root of *Chebyshev* node formula, as reported in Sect.3.2. In Fig. 15(a) the grey rectangles represent the L9 sub-domains but the points of each sub-domain are not reported to not weigh down the figure. Similarly, in Fig. 15(b), the 20 B4 structural elements are shown but only the shared nodes between the elements are represented.

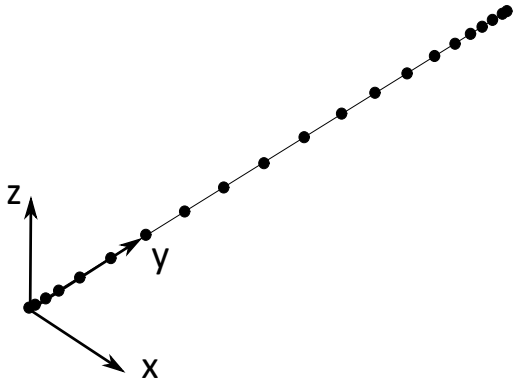

(a) Structural mesh along the beam axis - 20 B4

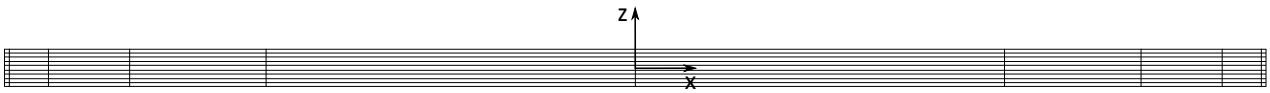

(b) Sub-domain distribution over the cross-section

Figure 15: Structural mesh along the beam axis and sub-domain distribution over the cross-section of the local 1D *CUF* model.

This benchmark is used to demonstrate that the global/local analysis in the CUF framework can detect the in-plane stresses in accordance with the global 2D model in *Msc-Nastran* and it can also describe of the

out-plane stress that can not be obtained from the global model.

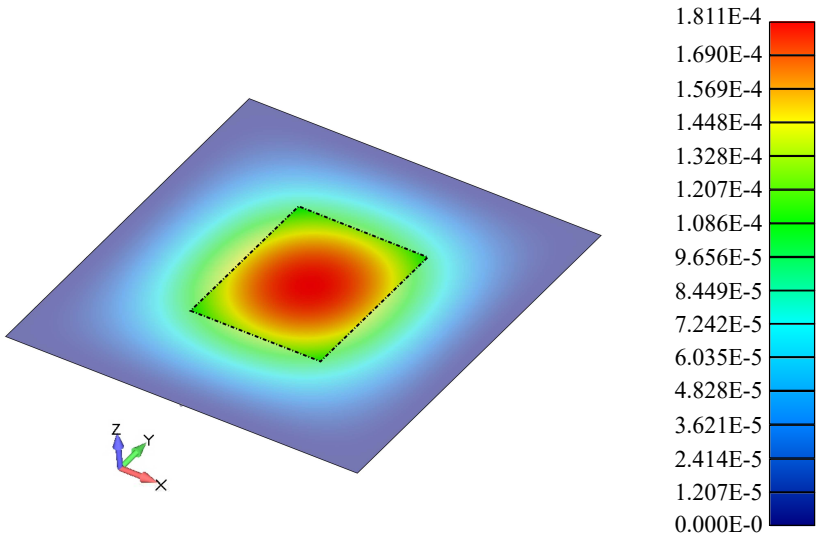

(a) Displacement magnitude in the global 2D model

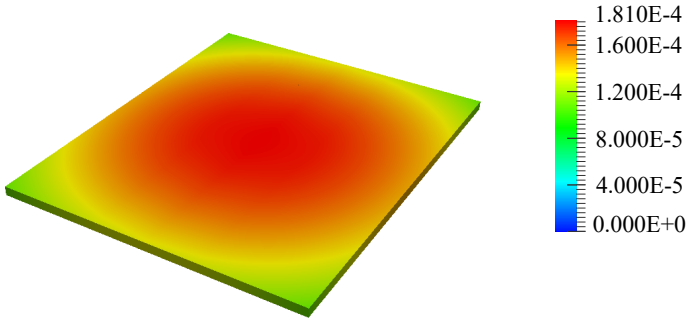

(b) Displacement magnitude in the local *CUF* model

Figure 16: Comparison between the global model and the global/local model in the displacement magnitude in mm

Figure 16 shows the displacement field magnitude in the global and in the local CUF model, while the axial stress σ_{yy} distribution through the thickness at the point A of the plate is presented in Fig. 17.
The shear stresses σ_{xy} and σ_{yz} are computed it the point B and they are shown in Fig. 18.
From the obtained results, the following considerations arise:

- The benchmark represents a typical plate problem, where the characteristic length of the plate b is much larger than the thickness t. This structure can be easily studied with the FE method using plate elements and, in the case of stress analysis, the in-plane stresses can be detected with a reasonable level of accuracy. Due to underlying kinematic assumptions, plate elements based on the classical theories such as Kirchoff or Reissner-Mindlin are unable to detect out-of-plane stresses. A 3D global model is set but, for this particular case, the computational cost can be very high so for this problem, a global/local approach can be useful to detect the 3D stress field in the most critical subregions of the structure.

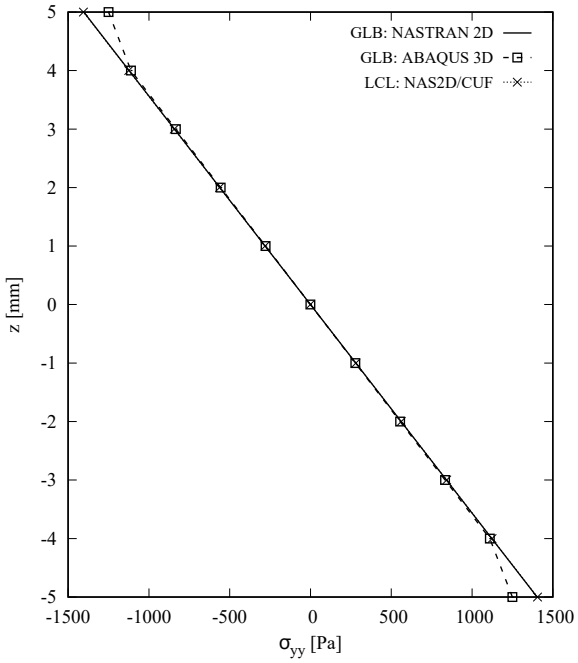

Figure 17: Axial stress σ_{yy} along the z-axis at the central point of the Plate, A

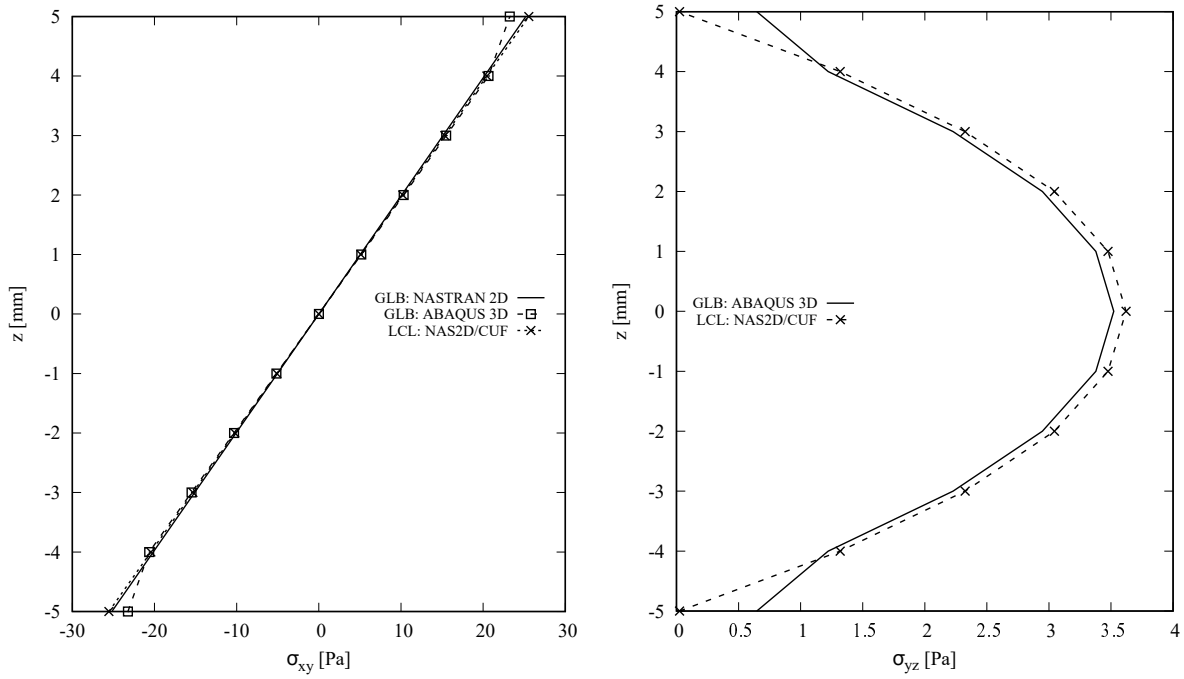

(a) Shear stress σ_{xy}

(b) Shear stress σ_{yz}

Figure 18: Shear stresses σ_{xy} and σ_{yz} along the z-axis for the local region of the isotropic plate. The stresses are computed at point B

- The global/local model detects correctly the results given by the global static analysis of the 2D model with the commercial software and provides the distribution of the out-plane stresses too. Figure 18(b) shows that the accuracy level of the global/local model is higher than the solid global model in the detection of the shear stress σ_{yz} in fact it correctly predicts the null value of σ_{yz} at the top and bottom of the cross-section.

- The computational cost of the global/local model in terms of DOFs, considering the static analyses of the global/local methodology, is 22326/107787 and it is one seventh of degrees of freedom required by the 3D model which are 855393.

4.3 Notched plate under uni-axial tension

This example is an application of the current global/local approach in the refined analysis of specific regions within a structure, where stress concentration is expected to occur. The structure is a plate of length $L = 150$ mm and width $W = 36$ mm with a central through hole of radius $R = 3$ mm, clamped at one end and subjected to a uniform displacement of $u_x = 0.025$ mm at the other end. A schematic representation of the structure, along with the applied BCs is given in Fig. 19.

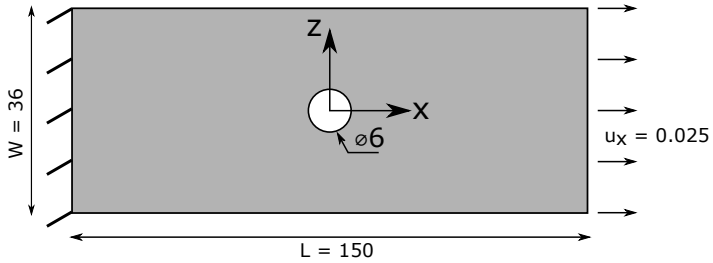

Figure 19: Schematic representation of the notched specimen along with the applied boundary conditions

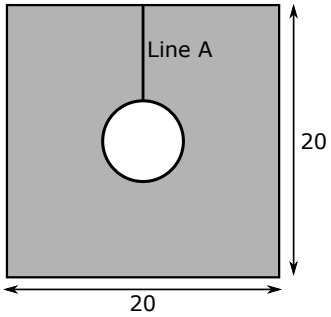

Figure 20: The local region considered for a refined analysis in CUF

In this example, a 3D ABAQUS coarse model is set up for the global analysis, whose displacements are then used to drive the local analysis in CUF. The region around the hole, where the maximum stresses are expected to occur, is considered to be the domain of the local analysis and is shown in Fig. 20.

A refined 3D analysis of the entire global structure has also been performed in ABAQUS, which constitutes a numerical reference solution. The mesh details of the various numerical models have been listed in Table 3. The results of the various analyses are presented hereinafter. The axial stress σ_{xx} along the line joining the points [x = 0.0, y = 1.25, z = 3.0] and [x = 0.0, y = 1.25, z = 10.0], i.e. the line A as shown in Fig. 20, has been plotted in Fig. 21.

Models	Mesh Type	DOFs
GLB: ABAQUS 3D (Ref.)	42120 C3D8	155898
LCL:ABQ3D/CUF	510 C3D8/1 B4 - 112 L9	2709/5760

Table 3: Mesh data for the numerical models used in the analysis of the notched specimen

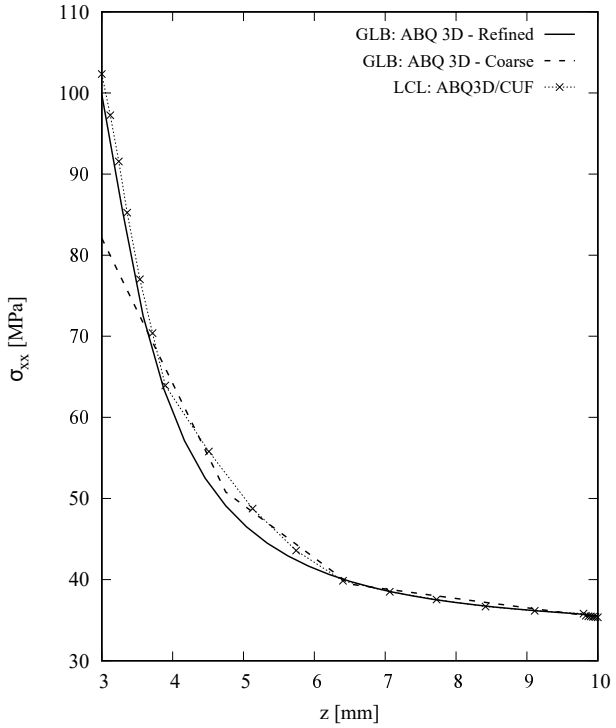

Figure 21: Axial stress σ_{xx} along the z axis

The following observations can be made:

1. A refined solution of the critical region can be found via the global/local approach, which requires about 18 times fewer DOFs with respect to a refined 3D finite element analysis.

2. From Fig. 21, it can be seen that accurate stresses can be obtained from the local CUF analysis without the need for extensive mesh refinement. This is due to the use of advanced structural theories within the CUF model.

3. Fig. 22 shows the axial stress σ_{xx} in the plane x-z comparing the global ABAQUS 3D models and the global/local one and confirming that this last could detect complex stress with a comparable accuracy to the refined 3D models. The plot of Fig. 22(b) is realized through an interface ABAQUS - CUF that permits to show the results of CUF local analysis using ABAQUS visualization tools.

4.4 Cantilever composite beam under bending

In this example, a composite beam with 3 plies is considered. The considered beam is clamped at one end and free at the other end, as described in [32].

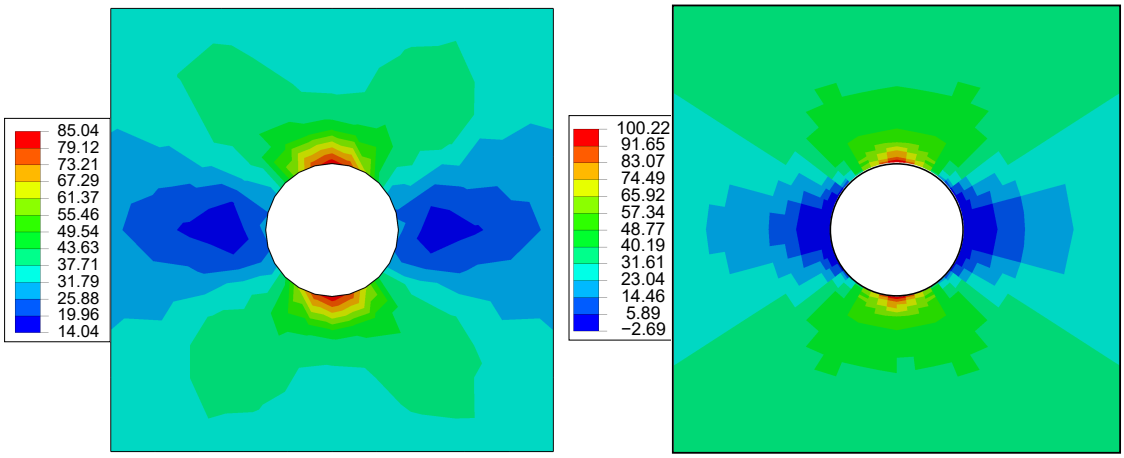

(a) ABAQUS 3D - Coarse

(b) Global - local CUF

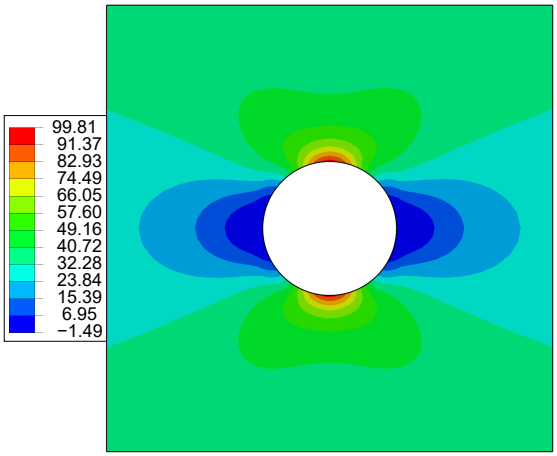

(c) ABAQUS 3D - Refined

Figure 22: Axial stress σ_{xx} $[MPa]$ in the plane x-z of the notched plate

The cross-section of the structure is presented in Fig. 23 and the structure is loaded by a point load along the z-direction at the centre of the free end and its magnitude is $-1 \cdot 10^{-3}$ N.

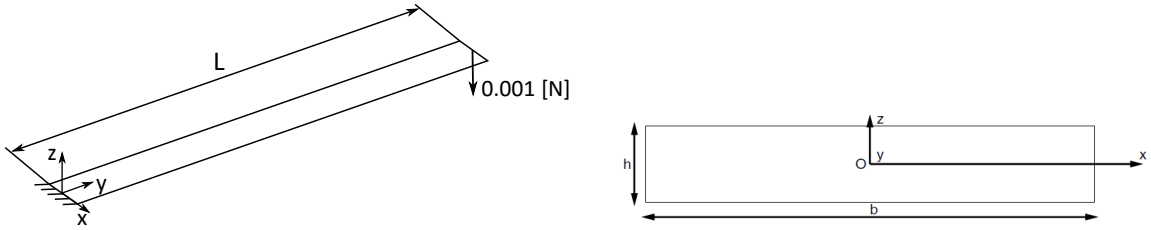

(a) Plate model

(b) Rectangular cross-section

Figure 23: Beam model and the geometrical features of its cross section

The geometrical characteristics of the structure are the length of $L = 2.0\ m$ and the cross-section width $b = 0.1$ m. The total thickness of the cross-section is $t = 0.003\ m$, the ply thickness is $t_{ply} = 0.001\ m$ and stacking sequence of the laminate is $[0°/90°/0°]$. An orthotropic material is taken into account with the following ma-

terial properties: $E_{11} = 40\ GPa$, $E_{22} = E_{33} = 4.0\ GPa$, $\nu_{12} = \nu_{13} = \nu_{23} = 0.25$, $G_{12} = G_{13} = G_{23} = 1.0\ GPa$. The global model is built in *MSc-Nastran* with a mesh of 10 x 200 plate elements.

The considered local region is a square region and constitutes a very small region within the global structure. It is located at the centre of the model and its geometrical parameters are $L_{local} = 10.0\ mm$, $b_{local} = 10.0\ mm$ $h_{local} = t = 3.0\ mm$. In the Fig. 24 the global structure is shown with the highlighted local region.

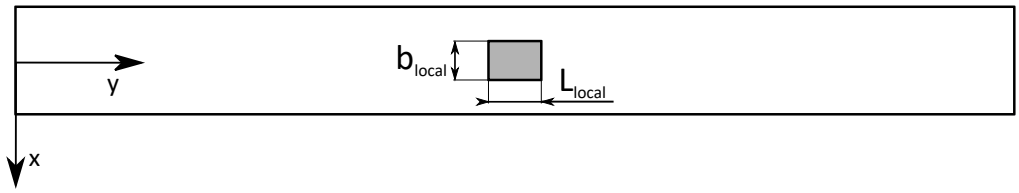

Figure 24: Global and local regions for the cantilever composite beam.

In the CUF local model 20 B4 structural beam elements are used along the y-axis direction and two different types of LE sub-domain distributions are adopted. The first one consists of 5x9 L9 sub-domains (5 along x and 9 along z) while the second one consists of 5x9 L16 sub-domains (5 along x and 9 along z) with 3 sub-domains for each layer of the structure.

The results of the static analysis are evaluated at the centre of the local region that is coincident with the global one.

In Fig. 25, the axial stress σ_{yy} and shear stress σ_{yz} distribution through the thickness are presented. The plot compares the results of the global analysis in *MSc-Nastran* with those of the global/local approach.

The following considerations can be done from the graphs reported in Fig. 25:

- For this benchmark, the commercial code always gives constant values of in-plane and out-plane stresses in each layer of the laminate. With the global/local approach, it is possible to detect the real trend of all the stresses.

- In Fig. 25(a), it can be noticed that both the global/local models catch the linear behaviour of the axial stress through the thickness of each layer and the results of the global/local model coincide with those of the global one only in the middle of each layer. As known, the commercial code gives just the average stress value of each layer.

- In Fig. 25(b), it can be noticed that both global/local models capture the quadratic behaviour of the shear stress. In particular, the global/local model with 5x9 L16 sub-domains is able to predict the null value of the σ_{yz} at the top and bottom of the cross-section

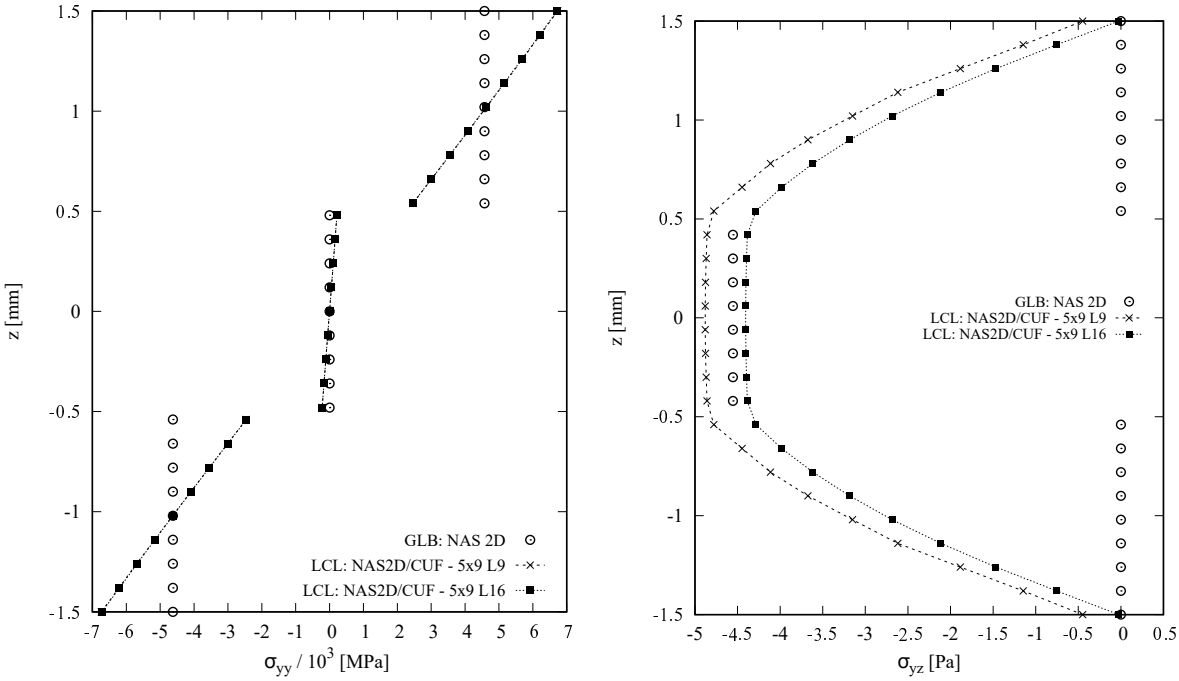

(a) Axial stress σ_{yy}

(b) Shear stress σ_{yz}

Figure 25: Axial stress σ_{yy} and Shear stress σ_{yz} along the z-axis for the cantilever composite beam

5 Conclusions

A global/local approach is necessary when a complex structure requires a detailed stress analysis in critical regions. In this work, a two-step methodology has been developed for Global/Local stress analysis in the CUF framework. In the first step, a preliminary static analysis on the 1D/2D model by using software (i.e. *MSc-Nastran, Abaqus CAE*) is done for obtaining all the necessary information for the pre-processing phase of the Local model. The second step is devoted to the static analysis of the local high order 1D *CUF* model using geometrical BCs at the interface level. Several numerical meaningful benchmarks have been proposed to assess the validity of the methodology, which is able to compute accurate 3D stress fields in the domain of the local region by significantly reducing the computational burden with respect to detailed local models made of 3D solid elements. Further developments of the methodology are under examination, as non-linear local analyses and localized buckling with the possibility to couple the global/local methodology with optimization tools for optimizing restricted (specified) areas of the global model, in order to reduce processing time.

References

[1] I. Babuška, J. Chandra, J. E. Flaherty, Adaptive computational methods for partial differential equations, Vol. 16, Siam, 1983.

[2] B. Szabó, I. Babuška, Finite element analysis, Wiley, New York, 1991.

[3] K.-J. Bathe, Finite element procedures, Klaus-Jurgen Bathe, 2006.

[4] J. Fish, L. Pan, V. Belsky, S. Gomaa, Unstructured multigrid method for shells, International Journal for Numerical Methods in Engineering 39 (7) (1996) 1181–1197.

[5] N. Moës, J. Dolbow, T. Belytschko, A finite element method for crack growth without remeshing, International Journal for Numerical Methods in Engineering 46 (1) (1999) 131–150.

[6] J. Fish, The s-version of the finite element method, Computers & Structures 43 (3) (1992) 539–547.

[7] J. Fish, S. Markolefas, Adaptive s-method for linear elastostatics, Computer Methods in Applied Mechanics and Engineering 104 (3) (1993) 363–396.

[8] K. W. Shim, D. J. Monaghan, C. G. Armstrong, Mixed dimensional coupling in finite element stress analysis, Engineering with Computers 18 (3) (2002) 241–252.

[9] P. Blanco, R. Feijóo, S. Urquiza, A variational approach for coupling kinematically incompatible structural models, International Journal for Numerical Methods in Engineering 197 (17-18) (2008) 1577–1602.

[10] K. Mao, C. Sun, A refined global-local finite element analysis method, International Journal for Numerical Methods in Engineering 32 (1) (1991) 29–43.

[11] H. B. Dhia, Multiscale mechanical problems: the Arlequin method, Comptes Rendus de l'Academie des Sciences Series IIB Mechanics Physics Astronomy 12 (326) (1998) 899–904.

[12] H. Hu, S. Belouettar, M. Potier-Ferry, et al., Multi-scale modelling of sandwich structures using the Arlequin method part i: Linear modelling, Finite Elements in Analysis and Design 45 (1) (2008) 37–51.

[13] F. Biscani, G. Giunta, S. Belouettar, E. Carrera, H. Hu, Variable kinematic beam elements coupled via arlequin method, Composite Structures 93 (2) (2011) 697–708.

[14] R. J. Guyan, Reduction of stiffness and mass matrices, AIAA Journal 3 (2) (1965) 380–380.

[15] M. Nastran, Superelement users guide, MSC. Software Corporation.–2001.–72 .

[16] J. B. Ransom, N. F. Knight Jr, Global/local stress analysis of composite panels, Computers & Structures 37 (4) (1990) 375–395.

[17] R. K. Kapania, S. G. Haryadi, R. T. Haftka, Global/local analysis of composite plates with cutouts, Computational Mechanics 19 (5) (1997) 386–396.

[18] S. Haryadi, R. Kapania, R. Haftka, Global/local analysis of composite plates with cracks, Composites Part B: Engineering 29 (3) (1998) 271–276.

[19] D. Muheim Thompson, O. Hayden Griffin JR, 2-d to 3-d global/local finite element analysis of cross-ply composite laminates, Journal of Reinforced Plastics and Composites 9 (5) (1990) 492–502.

[20] E. Carrera, A. Pagani, M. Petrolo, Use of Lagrange multipliers to combine 1d variable kinematic finite elements, Computers & Structures 129 (2013) 194–206.

[21] E. Zappino, G. Li, A. Pagani, E. Carrera, Global-local analysis of laminated plates by node-dependent kinematic finite elements with variable esl/lw capabilities, Composite Structures 172 (2017) 1–14.

[22] E. Carrera, M. Filippi, P. Mahato, A. Pagani, Accurate static response of single-and multi-cell laminated box beams, Composite Structures 136 (2016) 372–383.

[23] E. Carrera, M. Cinefra, M. Petrolo, E. Zappino, Finite element analysis of structures through unified formulation, John Wiley & Sons, 2014.

[24] I. Kaleel, M. Petrolo, E. Carrera, Elastoplastic and progressive failure analysis of fiber-reinforced composites via an efficient nonlinear microscale model, Aerotecnica Missili & Spazio 97 (2) (2018) 103–110.

[25] E. Carrera, I. Kaleel, M. Petrolo, Elastoplastic analysis of compact and thin-walled structures using classical and refined beam finite element models, Mechanics of Advanced Materials and Structures (2017) 1–13.

[26] M. Petrolo, M. Nagaraj, I. Kaleel, E. Carrera, A global-local approach for the elastoplastic analysis of compact and thin-walled structures via refined models, Computers & Structures 206 (2018) 54–65.

[27] E. Carrera, G. Giunta, M. Petrolo, Beam structures: classical and advanced theories, John Wiley & Sons, 2011.

[28] M. NASTRAN, Reference manual, 2008, MSC Software Corporation.

[29] J. J. Wijker, Mechanical vibrations in spacecraft design, Springer Science & Business Media, 2004.

[30] L. Liao, A study of inertia relief analysis, in: 52nd AIAA/ASME/ASCE/AHS/ASC Structures, Structural Dynamics and Materials Conference 19th AIAA/ASME/AHS Adaptive Structures Conference 13t, 2011, p. 2002.

[31] A. R. Barnett, T. W. Widrick, D. R. Ludwiczak, Closed-form static analysis with inertia relief and displacement-dependent loads using a msc/nastran dmap alter.

[32] E. Carrera, M. Petrolo, Refined one-dimensional formulations for laminated structure analysis, AIAA Journal 50 (1) (2012) 176–189.